

## Homogenization Function of Microchannel on Heat Absorber with Compound Parabolic Concentrator

WANG Xueqing, WU Haifeng, MA Yusen, WANG Suilin, XU Rongji\*

Beijing Engineering Research Center of Sustainable Energy and Buildings, Beijing University of Civil Engineering and Architecture, Beijing 100044, China

© Science Press, Institute of Engineering Thermophysics, CAS and Springer-Verlag GmbH Germany, part of Springer Nature 2022

**Abstract:** Microchannels offer unique advantages on heat transfer performance. In this paper, microchannels are applied to the compound parabolic concentrator (CPC) system. A multi-physical field coupling model based on Finite Element Method is proposed to investigate the homogenization effect of the microchannel heat absorber on the CPC non-uniform concentration. The energy conversion process from optics to heat is simulated using TracePro software, and the heat transfer processes in the microchannel are computed by Fluent using user defined functions (UDF). It is found that the microchannels behave well on weakening the influence of the nonuniformity solar heat flux on the performance of the CPC. The temperature nonuniformity of the outlet section is less than  $10^{-3}$  in the direction of fluid flow caused by the microchannel, although the maximum surface heat flux inhomogeneity of the microchannel reaches 2.3. The peak value of the heat flux on the surface of the absorber changes from double peak to single peak, and moves to the edge, resulting in more uneven heat flux distribution with the increase of the incident angle within the acceptance semi-angle of the CPC. The result of TracePro clearly shows that when the concentration ratio is less than 5, the heat flux nonuniformity on the surface of the absorber decreases with the increase in concentration ratio. It was interestingly found that the temperature distribution of the heat transfer fluid has weak sensitivity to the changes of truncation ratio. This work provides a way to design a CPC solar collector.

**Keywords:** solar energy, microchannel, compound parabolic concentrator, multi-physical field

### 1. Introduction

The compound parabolic concentrator (CPC) has been extensively studied on the design principles and concentrating characteristics in recent years [1]. The non-uniform heat flux distribution is formed on the surface of the heat absorber due to the optical property of the CPC [2–4], and it leads some negative effects on the CPC system, such as temperature non-uniform distribution, high thermal stresses, rapid aging of the heat

absorber, restraining the improvement of the heat collection efficiency [5].

With respect to the problems of non-uniform heat flux distribution, many scholars have carried out many works in recent years. In order to acquire uniform heat flux in the actual conditions, different CPC structures are proposed as they change the light distribution from the concentrator. Some CPCs integrate an air layer inside the reflector, where maximizes total internal reflection and obtains more homogeneous heat flux [6]. Zhang et al. [7]

<b>Nomenclature</b>			
$a$	the aperture width of CPC/m	$p$	fluid pressure/Pa
$C$	concentration ratio	$s$	the width of microchannel absorber/m
$C_t$	truncation ratio	$T$	the temperature of working fluid/K
$f$	parabolic focal length/m	$u$	the velocity/ $\text{m}\cdot\text{s}^{-1}$
$H$	the vertical distance from the aperture to the starting point of profile CPC/m	<b>Greek symbols</b>	
	the vertical distance from the aperture to the starting point of profile after CPC truncation/m	$\alpha$	thermal diffusivity of fluid of working/ $\text{m}^2\cdot\text{s}^{-1}$
$H_t$		$\theta$	the incident angle/( $^\circ$ )
$i$	data serial number	$\theta_{\max}$	the acceptance semi-angle of CPC/( $^\circ$ )
$K$	uniformity	$\rho$	density of working fluid/ $\text{kg}\cdot\text{m}^{-3}$
$M$	the arithmetic mean of data	$\sigma$	the standard deviation of the data
$n$	the number of data		

proposed a biaxial tracking CPC with a special truncation ratio. It is noticed that the non-uniform of heat flux is reduced to about 27% compared with that of an ordinary CPC according to Monte-Carlo ray tracing simulations. He et al. [5] used a secondary mirror to optimize CPC geometry, which shows a homogenized energy flow distribution on the out wall of the absorber. These problems are relatively under studied among CPC collectors, though there have been many studies on trough collectors. Our work is also inspired by the recent progresses in trough collectors. Geng et al. [8] analyzed the thermal stress of the absorber in the trough collector under the non-uniform heat flux density. The high inlet temperature and the larger flow rate of the working fluid are suggested to reduce the thermal stress of the absorber. But it is difficult to obtain smaller thermal stress by changing working conditions in practical applications. An alternative way for homogenization heat flux is to change the absorber. For example, Peng et al. [9] optimized the heat flux distribution by changing the structure of the absorber. They inserted gradient metal foam into the heat absorber, and the experiment shows the partially filled tube had more temperature uniformity and less thermal stress than that of the empty tube. However, the complicated structures will make the processing more difficult. The fluid inside the heat absorber also affects the distribution of heat flux. Nabeel et al. [10] and Ying et al. [11] showed that the maximum temperature of the absorber can be reduced when changing different working fluids. Another important consideration in homogenization heat flux is changing the material of the absorber. Akbarimosavi et al. [12] found the peripheral temperature difference of the absorber reduces when using the high thermal conductivity material. Similar findings were reported by Aldali et al. [13] for aluminum absorbers. They observed that the circumferential thermal gradient of the aluminum absorber was significantly

smaller than that of the steel absorber, indicating that the materials with relatively large thermal conductivity can alleviate the non-uniform energy distribution. Robles et al. [14] used the aluminum microchannel absorber in the flat plate collector. The microscale channels are also used to improve the performance of the solar system. Zhou et al. [15] used minichannels in solar photovoltaic-thermal system to improve the overall performance of the system. Sharma et al. [16] proposed the use of minichannels in evacuated-tube solar collector as absorber and established a heat transfer model. They found that this kind of collector has higher thermal efficiency than the evacuated-tube solar collector. However, they did not elaborate more about the non-uniform heat flux on the surface of the heat absorber, which is caused by CPC concentrating characteristics.

The microchannel has the advantages of the simple structure, low price [17, 18], high stability and good thermal performance [19], which is widely used in micro-electronic mechanical and electronic devices systems [20]. The aluminum microchannel is promising to alleviate the influence of the non-uniform heat flux distribution on the absorber. Therefore, this paper proposes a CPC solar collector with the microchannel absorber and investigates the homogenization function of the microchannel under the CPC concentrating characteristics. The main works are summarized as follows:

Firstly, a novel CPC solar collector with microchannel absorber was designed with specific structural parameters. Based on Finite Element Method, a multi-physical field coupling model was introduced to study the homogenization effect of the microchannel heat absorber on CPC non-uniform concentration. Then, the non-uniform heat flux distribution on the surface of the microchannel heat absorber formed by the CPC concentrator at different incidence angles, concentration

ratios and truncation ratios was calculated. The temperature distribution of the microchannel heat absorber under different working conditions was further modeled and discussed. Finally, the homogenization effect of the microchannel on heat absorber with the CPC was analyzed. This paper provides a promising way for improving the performance of the solar CPC absorber.

## 2. CPC with Microchannel Heat Absorber

### 2.1 Design of the CPC and the microchannel heat absorber

The CPC solar collector with microchannels is composed of CPCs, a microchannel heat absorber, an inlet pipe, an outlet pipe, an insulation layer, a glass cover plate and a collector shell, as shown in Fig. 1. The length and width of the collector are 2 m and 1 m, as the same as those of the conventional flat plate solar collector, which is more conducive to building integration. The schematic diagram of the section structure is shown in Fig. 2. The insulation layer is under and around the CPC and the microchannel. Through the glass cover plate, part of the sunlight directly reaches the microchannel heat absorber, and another part reaches the microchannel heat absorber through CPC reflection. The microchannel heat absorber is heated by the light irradiation and then heats the circulating working fluid in the microchannel. To simplify the model and explore the concentrating properties of the CPC, the concentrator unit composed of the CPC and the microchannel absorber was selected as the research object.

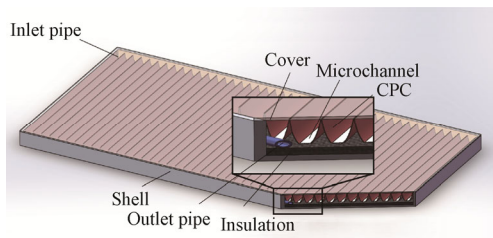


**Fig. 1** Schematic diagram of the CPC microchannel solar collector

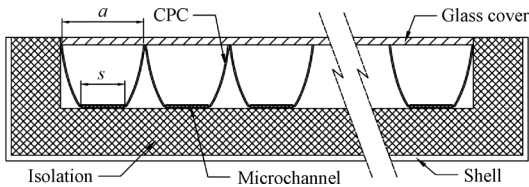


**Fig. 2** Schematic diagram of the CPC microchannel solar collector section structure

The CPC is composed of two parabolas symmetrical on the left and right sides [21], as shown in Fig. 3. The concentration ratio  $C$  of the CPC is defined as follows:

$$C = \frac{1}{\sin(\theta_{\max})} = \frac{a}{s} \quad (1)$$

where  $\theta_{\max}$  can be gained when  $C$  is given. The truncation ratio  $C_t$  of the CPC is defined as follows:

$$C_t = H_t/H \quad (2)$$

The profile equation on the right side of the CPC is expressed as:

$$y = x^2/4f \quad (3)$$

The parabolic focal length is:

$$f = \frac{s}{2}(1 + \sin \theta_{\max}) \quad (4)$$

The starting point coordinates of the right profile of the CPC are:

$$\begin{cases} x_s = s \cos \theta_{\max} \\ y_s = \frac{s}{2}(1 - \sin \theta_{\max}) \end{cases} \quad (5)$$

The coordinates of the ending point of the profile are:

$$\begin{cases} x_f = (s + a) \cos \theta_{\max} \\ y_f = \frac{s}{2}(1 - \sin \theta_{\max}) \left(1 + \frac{1}{\sin \theta_{\max}}\right)^2 \end{cases} \quad (6)$$

The connecting line between the starting point of the right profile of the CPC and the focus of parabola is the position of the microchannel absorber. The vertical line is the central axis of the CPC. The left and right profiles of the CPC are symmetrical about the central axis passing through the midpoint of the connecting line, as shown in Fig. 3.

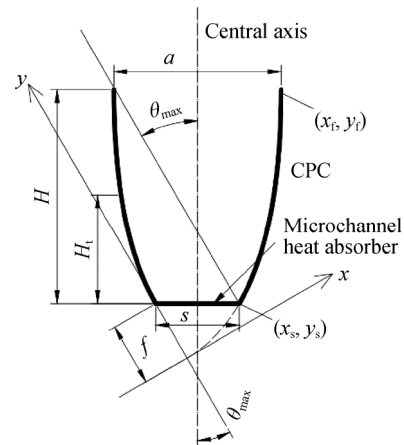


**Fig. 3** Schematic diagram of the CPC

The microchannel heat absorber made of aluminum consists of 11 parallel microchannel channels with a length of 1 m. As depicted in Fig. 4, the cross-sectional size of each channel is 1.2 mm×0.6 mm and the distance between each flow path is 0.2 mm. The cross-sectional size of the whole microchannel component is 16 mm in width and 1.4 mm in height.

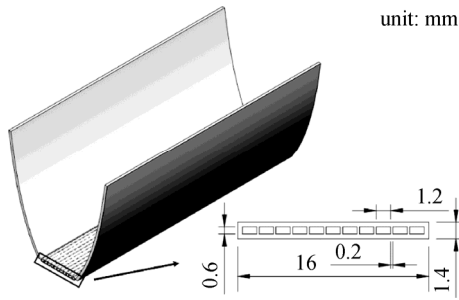


Fig. 4 Geometry of the CPC microchannel

## 2.2 Surface heat flux simulation of the microchannel heat absorber

To obtain the heat flux distribution of the microchannel absorber, the equal proportion concentrating model is established to simulate the light by TracePro software. To simplify the model, the following assumptions and settings were made: (1) the reflectivity of the CPC surface was 0.9; (2) the surface absorptivity of the microchannel heat absorber was 0.85; (3) the simulated light source was set as surface light source; (4) the light source of radiation simulation was set as the sunshine distribution; (5) the total number of rays was set to 10 000; (6) the value of solar radiation intensity was set to  $1000 \text{ W/m}^2$ ; (7) the light energy level was distributed to each photon; (8) the light reflection along the flow direction of the microchannel was considered as completely consistent; (9) the influence of season and other factors on solar radiation intensity was neglected.

Based on the model in TracePro, the number of reflected lights and the coordinates of photons falling on the microchannel absorber could be obtained. The energy carried by each photon was calculated according to the intensity of solar radiation and the area of the light source. The distribution density of photons on the surface of the heat absorber, and the heat flux density distribution on the surface of the microchannel absorber were calculated by MATLAB software.

To verify the reliability of the model, the working condition was set to be consistent with that in the published work [22]. The concentration ratio, truncation ratio and reflectivity of the CPC were 1.6, 0.5 and 0.8, respectively. The length of the absorber, the absorber surface absorptivity and the incident angle of light were 0.2 m, 0.9 and  $0^\circ$ , respectively. The heat flux distribution under the condition obtained by the model in this work was compared with that based on experimental and simulation data in Ref. [22], as shown in Fig. 5. It is found the result achieved from the model fits well with that of previous work, verifying the effectiveness of the theoretical model.

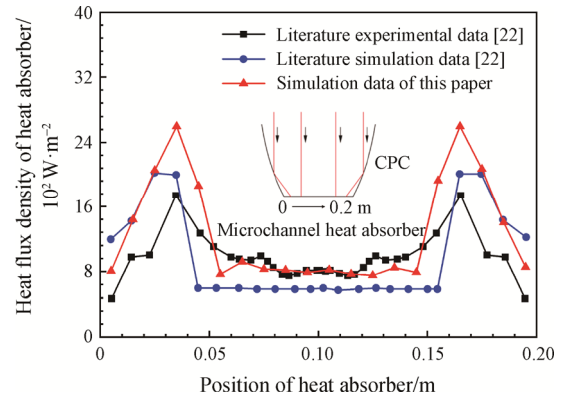


Fig. 5 Comparison of the heat flux distribution obtained by the model in this work and Ref. [22] under the same conditions

## 2.3 Numerical simulation of the microchannel absorber

Newton fluid satisfies three laws of mass conservation, momentum conservation and energy conservation as follows [23, 24]. Given the initial conditions and the boundary conditions, the velocity field and the temperature field can be obtained by solving the three equations. The continuity equation is as follow:

$$\frac{\partial(\rho u_i)}{\partial x_i} = 0 \quad (7)$$

The momentum equation is as follow:

$$\frac{\partial}{\partial x_i}(\rho u_i u_j) = -\frac{\partial p}{\partial x_i} + \frac{\partial}{\partial x_j} \left[ (\mu_t + \mu) \left( \frac{\partial u_i}{\partial x_j} + \frac{\partial u_j}{\partial x_i} \right) - \frac{2}{3} (\mu_t + \mu) \delta_{ij} \frac{\partial u_l}{\partial x_l} \right] + \rho g_i \quad (8)$$

where  $\mu$  is the kinetic viscosity, Pa·s.  $\mu_t$  is the eddy viscosity, Pa·s.  $\delta_{ij}$  is the Kronecker delta. The items in Eq. (8) square bracket indicate the stress tensor, and  $\rho g_i$  is the gravitational body force.

The energy equation is as follows:

$$\frac{\partial}{\partial x_i}(u_i T) = \frac{\partial}{\partial x_i} \left( \alpha \frac{\partial T}{\partial x_i} \right) \quad (9)$$

Gambit software was used to mesh the microchannel heat absorber model. The mesh division diagram of the microchannel heat absorber is shown in Fig. 6. To obtain more accurate results, the minimum wall was designed as two layers of mesh. After inspection, the minimum orthogonal quality is 0.99, which is also beneficial for the simulation process. In order to verify the accuracy and reliability of the simulation results, the mesh independence was carried out with four mesh cases (as shown in Fig. 7). It can be seen that when the mesh increases from 3 580 000 to 12 600 000, the fluid outlet temperature changes only 0.39%. Therefore, the meshes in Fig. 6 were found to be sufficient for the present study.

The mesh of the microchannel heat absorber was imported into Fluent. Water was used as working fluid. The inlet temperature and velocity of the working fluid were defined as 300 K and 0.02 m/s, respectively. The non-uniform heat flux formed by the CPC concentrating was set as heat flux boundary at the heat absorbing surface (upper wall) of the microchannel absorber by User-Defined-Functions (UDF). The other surfaces of the absorber were set as adiabatic boundary conditions.

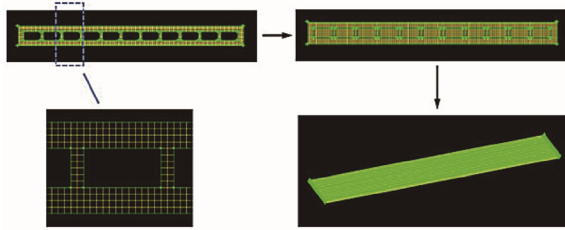


Fig. 6 Mesh division diagram of the microchannel heat absorber

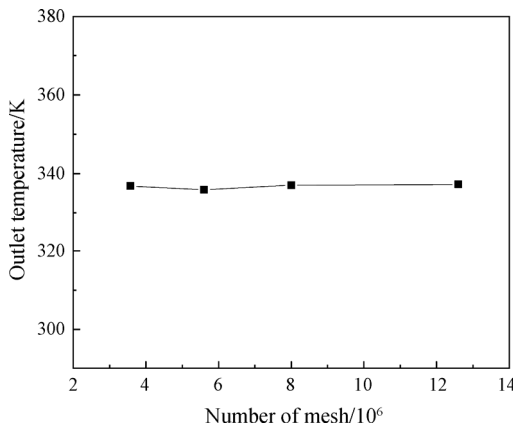


Fig. 7 Fluid outlet temperature with four different meshes for microchannel

**2.4 Nonuniformity calculation and calculation condition**

Nonuniformity is defined to study the uniformity of temperature and heat flux distribution on the surface of the microchannel heat absorber. Mathematically, the nonuniformity  $K$  is the coefficient of variation. It is suitable to use the coefficient of variation compare variation among dissimilar things [25]. The smaller the value of the  $K$ , the better the uniformity [26]. Namely nonuniformity  $K$  is the ratio of the standard deviation of the data  $\sigma$  to the arithmetic mean  $\bar{M}$  [27] as expressed:

$$K = \sigma / \bar{M} \tag{10}$$

The arithmetic mean and standard deviation of the data are calculated as:

$$\bar{M} = \frac{1}{n} \sum_{i=1}^n M_i \tag{11}$$

$$\sigma = \sqrt{\frac{\sum_{i=1}^n (M_i - \bar{M})^2}{n - 1}} \tag{12}$$

The incidence angle, concentration ratio and truncation ratio are three important factors in the design of CPC collectors. In order to verify the good homogenization effect of microchannels, the CPC collector was tested under different working conditions by changing the above three factors. The calculation conditions are shown in Table 1.

Table 1 Simulation conditions

Case	Incident angle/(°)	Concentrating ratio	Truncation ratio
1	0, 10, 20, 29, 40	2	0.5
2	0	2, 3, 4, 5, 6	0.5
3	0	2	0.3, 0.5, 0.7

**3. Results and Discussion**

**3.1 Influence of the incident angle on the homogenization effect of microchannels**

The heat absorption characteristics of the microchannel heat absorber at different incident angles were simulated. The intersection position of the microchannel heat absorber and the CPC is left in 0 mm and right in 16 mm. As shown in Fig. 8, the non-uniform heat flux distribution is formed on the surface of the microchannel due to the concentrating properties. As shown in Fig. 9, the value of the peak gradually increases with the increase of the incident angle within the CPC acceptance semi-angle (30°). It makes the heat flux distribution more non-uniform on the surface of the microchannel (as shown in Fig. 10). When the incident angle is close to the maximum acceptance semi-angle of the CPC, the peak value of heat flux density reaches 22 600 W/m<sup>2</sup> (Fig. 9). The nonuniformity of heat flux distribution reaches 2.3 (Fig. 10). The temperature difference of the fluid in the enlarged detail does not exceed 2 K in this case (Fig. 11) showing the great homogenization function of microchannel. It can be attributed to the existence of baffles between microchannels, so that part of the heat is transferred from the heating surface to the relative inner surface through conduction. It makes the whole inner surface of each channel heated at the same time, thus enhancing the heat transfer. The temperature nonuniformity decreases gradually as the fluid flows through the microchannel. The temperature distribution at the outlet section of the microchannel is relatively uniform (see Fig. 10 and Fig. 11). The nonuniformity is no more than 4.4×10<sup>-4</sup>, which was smaller than that of heat flux nonuniformity. It is indicated that the homogenization effect of the microchannel absorber is good.

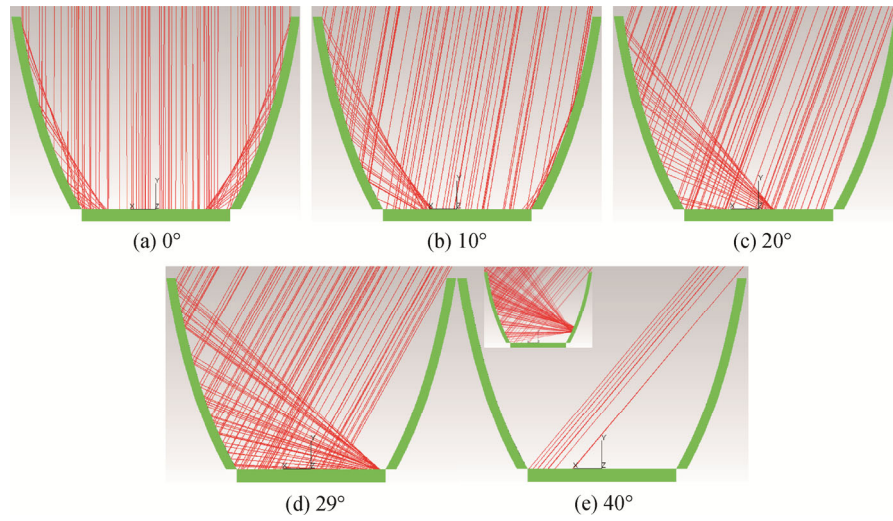


Fig. 8 Simulation of the light distribution at different incident angles

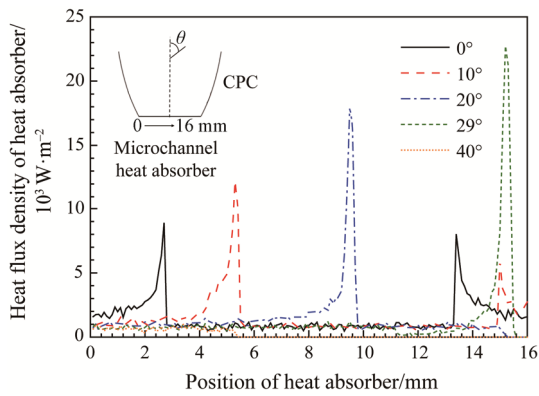


Fig. 9 Heat flux distribution at different incident angles

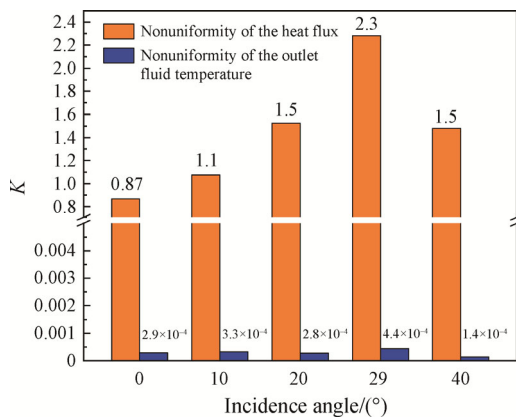


Fig. 10 Comparison of the surface heat flux density nonuniformity and the outlet section fluid temperature nonuniformity of the heat absorber at different incident angles

### 3.2 Influence of concentration ratio on the homogenization effect of microchannels

To gain further insights into the homogenization effect of the microchannel absorber, different concentration ratios were studied. Fig. 12 and Fig. 13 exemplify the

distribution of light and heat flux at different concentration ratios. Higher concentration ratio would boost the heat flux density on the surface of the microchannel absorber. As the concentration ratio increases, the position where the reflected light reaches the bottom of the microchannel heat absorber moves from both sides to the middle of the CPC.

As for the temperature distribution diagram of the microchannel absorber (see the enlarged detail in Fig. 14), the fluid temperature distribution is basically consistent with the heat flux distribution on the upper surface of the microchannel heat absorber. And the fluid temperature difference of the outlet is less than 0.82 K at different concentration ratios. The nonuniformity of the heat flux distribution on the upper surface of the microchannel absorber is the highest when the concentration ratio is 2. But the nonuniformity of the temperature distribution at the outlet section of the microchannel absorber is the lowest. The reason is that the bimodal value is small and the ratio of the bimodal value to the total heat flux is low. When the concentration ratio is 3, the nonuniformity of the fluid outlet temperature distribution reaches the maximum due to the larger heat flux bimodal value and larger ratio of the bimodal value to total heat flux. The main and secondary bimodal values are close to each other when the concentration ratio is greater than 3. So the temperature distribution uniformity of the microchannel outlet section has little difference. The temperature inhomogeneity decreases gradually when the fluid flows through the microchannel. And the temperature distribution at the outlet section of the microchannel is relatively uniform (less than 0.82 K) as indicated by Fig. 14. The value of the nonuniformity is less than  $9 \times 10^{-4}$ , which shows a great homogenization effect of the microchannel absorber (Fig. 15). The reason is ascribed that the high ratios of surface area to volume of microchannels and high thermal conductivity of

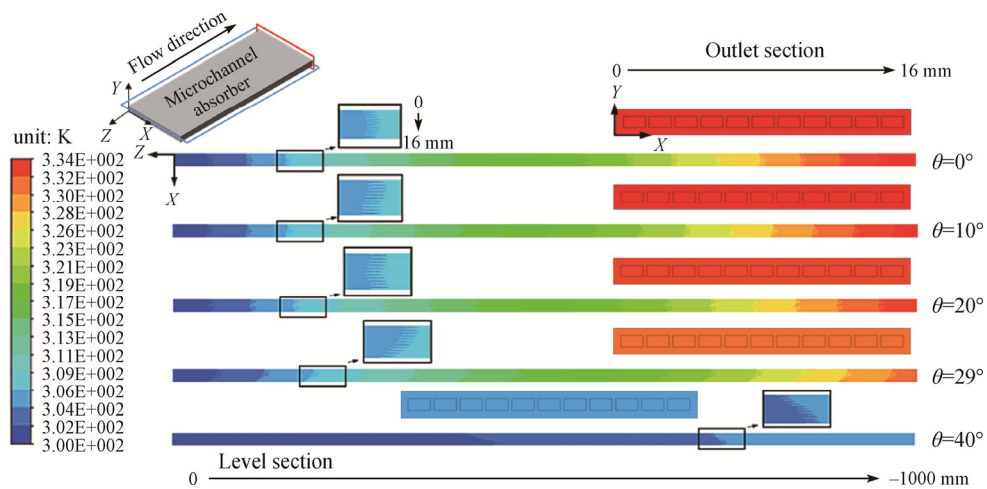


**Fig. 11** Temperature distribution of level section ( $y=0.7$  mm) and outlet section ( $z=-1000$  mm) at different incident angles

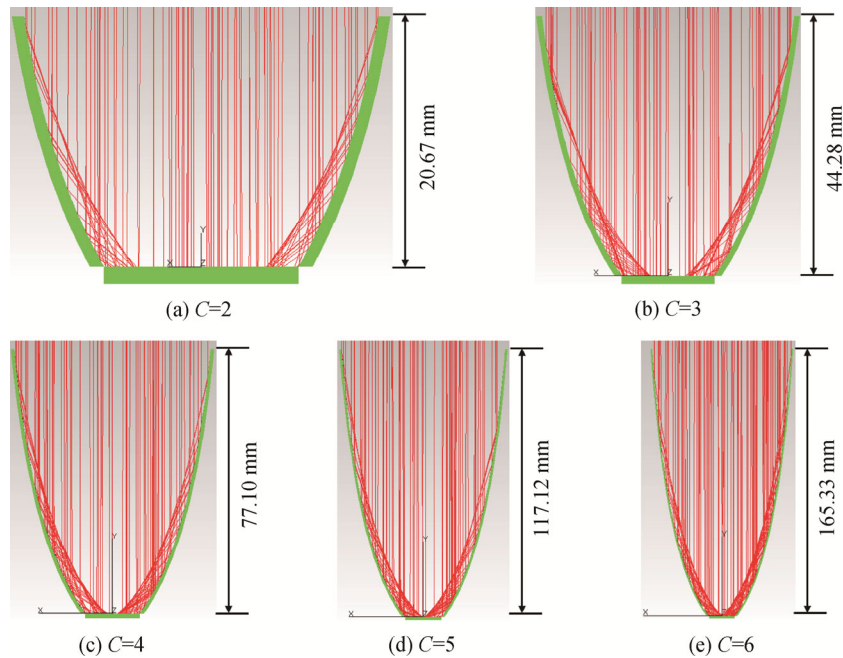


**Fig. 12** Simulation of the light distribution at different concentration ratios (the width of the microchannel absorber is 16 mm)

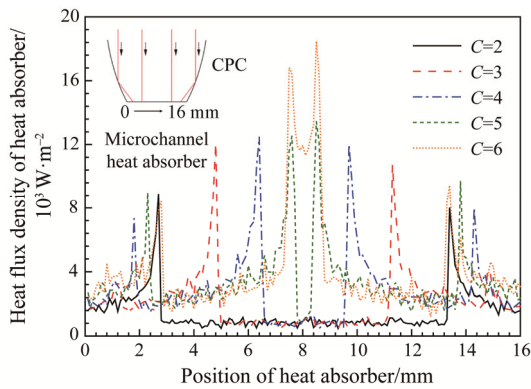


**Fig. 13** Distribution of the heat flux density at different concentration ratios

aluminum realize the thermal homogeneity across the absorber. The outlet temperature also increases with the increase of concentration ratio. It is indicated that the CPC with a higher concentration ratio can obtain higher fluid temperature rise in the same length heat absorber.

### 3.3 Influence of truncation ratio on the homogenization effect of microchannels

Truncation ratio is a necessary factor for gaining an efficient CPC solar collector. It is important to achieve the optimal solution with a higher collector temperature and lower cost. Thus the homogenization effect of microchannels at different truncation ratios was investigated. Fig. 16 and Fig. 17 respectively show the light tracing maps and the heat flux distribution maps of

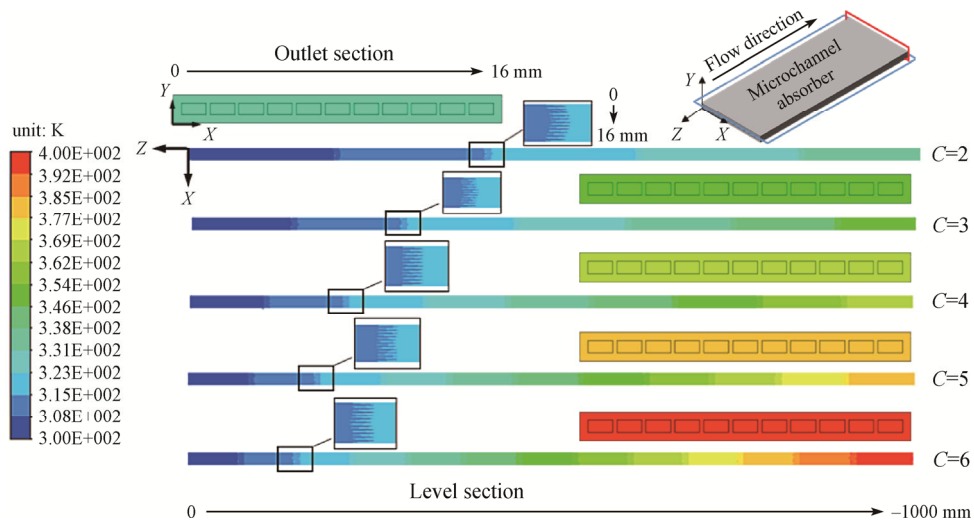


Fig. 14 Temperature distribution of level section ( $y=0.7$  mm) and outlet section ( $z=-1000$  mm) at different concentration ratios

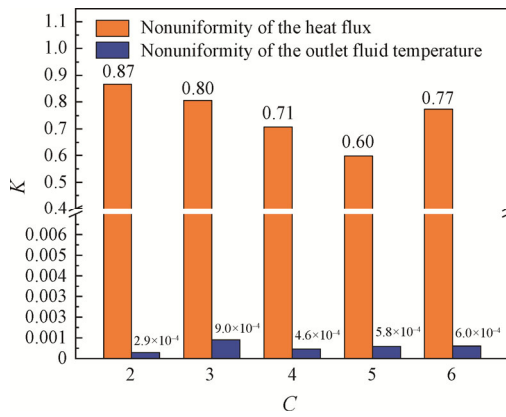


Fig. 15 Comparison of the surface heat flux density nonuniformity and the outlet section fluid temperature nonuniformity of the heat absorber at different concentration ratios

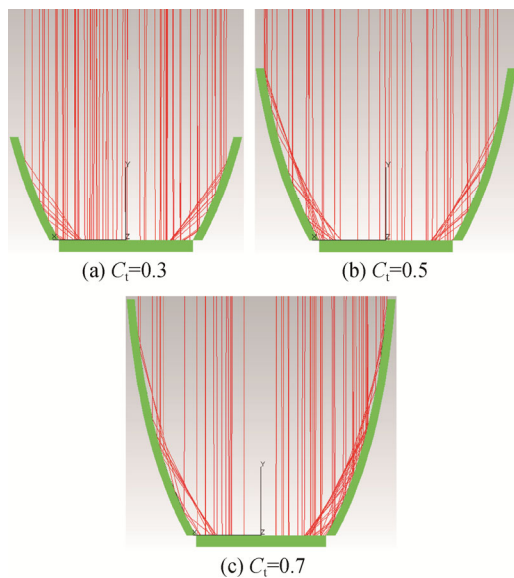


Fig. 16 Simulation of the light distribution at different truncation ratios

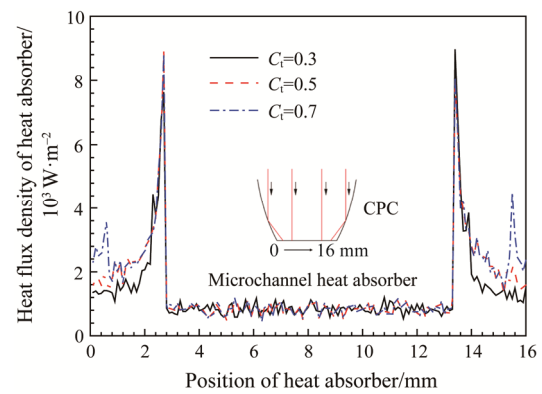


Fig. 17 Heat flux distribution at different truncation ratios

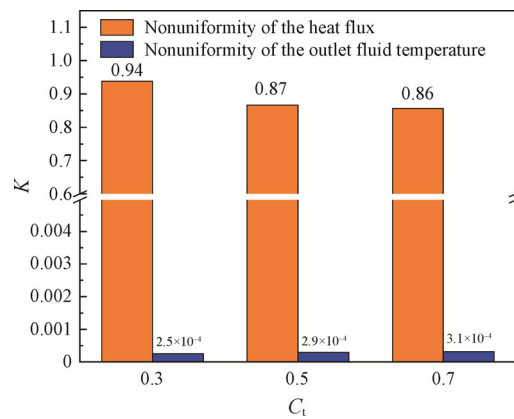
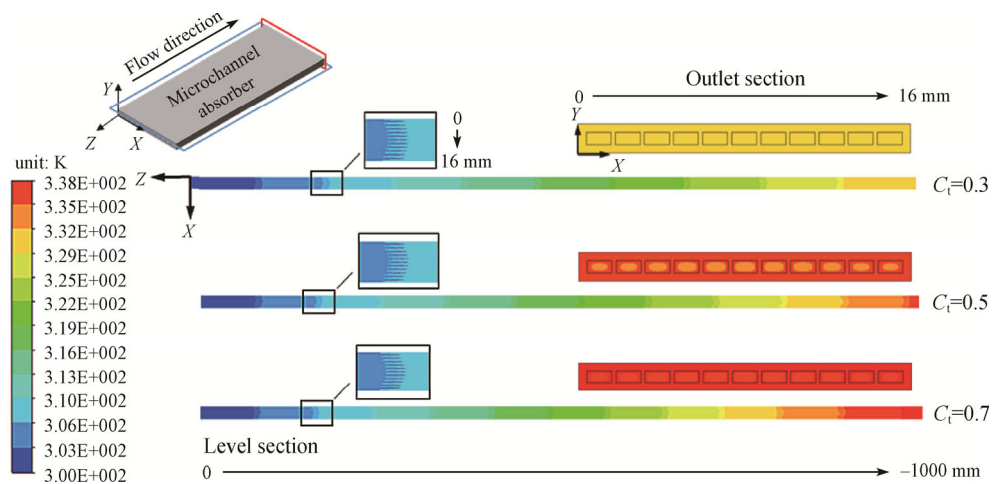


Fig. 18 Comparison of the surface heat flux density nonuniformity and the outlet section fluid temperature nonuniformity of the heat absorber at different truncation ratios

the concentrator unit with different truncation ratios. The distribution of the light reflected by the CPC on the surface of the microchannel absorber has little difference at different truncation ratios. It has a similar surface heat flux density nonuniformity, as shown in Fig. 18.





**Fig. 19** Temperature distribution of level section ( $y=0.7$  mm) and outlet section ( $z=-1000$  mm) at different truncation ratios

Fig. 19 shows that the fluid temperature distribution accords with the heat flux distribution on the outer surface of the microchannel absorber. As the fluid flows through the microchannel absorber, the temperature of the fluid increases gradually. The temperature difference at the outlet section is less than 0.4 K and the nonuniformity is less than  $3.1 \times 10^{-4}$  (as shown in Fig. 18), which are in good agreement with the fact that the microchannel heat absorber has a good homogenization function.

#### 4. Conclusions

Microchannels were used to weaken the nonuniformity solar heat flux due to the CPC optical characteristics in this paper. A multi-physical field coupling model is built to investigate the performances of the new CPC absorber, presenting the great homogenization function of the microchannel. The main conclusions are as follows:

(1) According to ray tracing method, the nonuniformity of the heat flux distribution on the surface of the microchannel heat absorber increases with the increase of the incident angle within the acceptance semi-angle of CPC. When the incident angle approaches the acceptance semi-angle of CPC, the maximum nonuniformity of both heat flux distribution and fluid outlet temperature distribution reaches the maximum. However, the temperature nonuniformity of the fluid outlet temperature at different incident angles is less than  $4.4 \times 10^{-4}$ . The homogenization of microchannel heat absorber is obvious.

(2) The nonuniformity of heat flux distribution on the surface of microchannel decreases with the increase of concentration ratio when the concentration ratio is less than 5. The reason is that the appearance of secondary bimodal homogenizes the heat flux distribution. There is

no positive correlation between the nonuniformity of fluid outlet temperature distribution and the nonuniformity of heat flux distribution. But the nonuniformity of fluid outlet temperature distribution is related to the heat flux distribution. When the concentration ratio is 2, the bimodal value is small and the ratio of the bimodal value to the total heat flux is low. So the nonuniformity of fluid outlet temperature distribution is the smallest under the homogenization effect of the microchannel. When the concentration ratio is 3, the bimodal value and the ratio of the bimodal value to total heat flux are larger, and the maximum nonuniformity of the fluid outlet temperature distribution is obtained. When the concentration ratio is greater than 3, there will be bimodal and secondary bimodal heat flux distribution. Under the effect of microchannel homogenization, the nonuniformity of fluid outlet temperature distribution is small.

(3) The truncation ratio has little effect on the nonuniformity of heat flux distribution and fluid outlet temperature distribution.

(4) The microchannel has outstanding homogenization function under all working conditions due to its special structure and high heat transfer coefficient.

#### Acknowledgements

This present study was supported by the National Natural Science Foundation of China (51506004), Beijing Scholars Program (2015No.022) and Fundamental Research Funds for Beijing University of Civil Engineering and Architecture (X20065).

#### References

- [1] Tian M., Su Y., Zheng H., et al., A review on the recent research progress in the compound parabolic concentrator

- (CPC) for solar energy applications. *Renewable and Sustainable Energy Reviews*, 2018, 82: 1272–1296.
- [2] Zhang G., Wei J., Wang Z., et al., Investigation into effects of non-uniform irradiance and photovoltaic temperature on performances of photovoltaic/thermal systems coupled with truncated compound parabolic concentrators. *Applied Energy*, 2019, 250: 245–256.
- [3] Meng H., The experimental and computational research on the intensity distribution of CPC absorber plate. *Acta Energetica Solaris Sinica*, 1996, 17(2): 151–156.
- [4] Ding H., Research on transfer characteristics of internal CPC vacuum solar thermal collector. Northeast Electric Power University, Jilin, China, 2017. (in Chinese)
- [5] He Y., Wang K., Du B., et al., Non-uniform characteristics of solar flux distribution in the concentrating solar power systems and its corresponding solutions: A review. *Science China Press*, 2016, 61(30): 3208–3237.
- [6] Li G., Pei G., Su Y., et al., Design and investigation of a novel lens-walled compound parabolic concentrator with air gap. *Applied Energy*, 2014, 125: 21–27.
- [7] Zhang H., Chen H., Han Y., et al., Experimental and simulation studies on a novel compound parabolic concentrator. *Renewable Energy*, 2018, 113: 784–794.
- [8] Geng C., Xue Q., Zhang W., et al., Thermal stress analysis for absorber tube of parabolic trough solar collector under non-uniform heat flux. *Journal of Engineering for Thermal Energy and Power*, 2019, 34(3): 121–127.
- [9] Peng H., Li M., Liang X., Thermal-hydraulic and thermodynamic performance of parabolic trough solar receiver partially filled with gradient metal foam. *Energy*, 2020, 211: 119046.
- [10] Nabeel A., Imran A., Andrea C., et al., Assessment and evaluation of the thermal performance of various working fluids in parabolic trough collectors of solar thermal power plants under non-uniform heat flux distribution conditions. *Energies*, 2020, 13(15): 1–27.
- [11] Ying Z., He B., Su L., et al., Convective heat transfer of molten salt-based nanofluid in a receiver tube with non-uniform heat flux. *Applied Thermal Engineering*, 2020, 181: 1–12.
- [12] Akbarimoosavi S.M., Yaghoubi M., 3D thermal-structural analysis of an absorber tube of a parabolic trough collector and the effect of tube deflection on optical efficiency. *Energy Procedia*, 2014, 49: 2433–2443.
- [13] Aldali Y., Muneer T., Henderson D., Solar absorber tube analysis: thermal simulation using CFD. *International Journal of Low-Carbon Technologies*, 2011, 8(1): 14–19.
- [14] Robles A., Duong V., Martin A.J., et al., Aluminum minichannel solar water heater performance under year-round weather conditions. *Solar Energy*, 2014, 110: 356–364.
- [15] Zhou J., Zhao X., Yuan Y., et al., Operational performance of a novel heat pump coupled with mini-channel PV/T and thermal panel in low solar radiation. *Energy and Built Environment*, 2020, 1(1): 50–59.
- [16] Sharma N., Diaz G., Performance model of a novel evacuated-tube solar collector based on minichannels. *Solar Energy*, 2011, 85(5): 881–890.
- [17] Widyolar B., Jiang L., Brinkley J., et al., Experimental performance of an ultra-low-cost solar photovoltaic-thermal (PVT) collector using aluminum minichannels and nonimaging optics. *Applied Energy*, 2020, 268: 1–11.
- [18] Wang Z., Huang Z., Chen F., et al., Experimental investigation of the novel BIPV/T system employing micro-channel flat-plate heat pipes. *Building Services Engineering Research and Technology*, 2018, 39(5): 540–556.
- [19] Li G., Zhang G., He W., et al., Performance analysis on a solar concentrating thermoelectric generator using the micro-channel heat pipe array. *Energy Conversion and Management*, 2016, 112: 191–198.
- [20] Zhou J., Cao X., Zhang N., et al., Micro-channel heat sink: a review. *Journal of Thermal Science*, 2020, 29(6): 1431–1462.
- [21] Rabl A., Optical and thermal properties of compound parabolic concentrators. *Solar Energy*, 1976, 18(6): 497–511.
- [22] Smyth M., Zacharopoulos A., Eames P.C., An experimental procedure to determine solar energy flux distributions on the absorber of line-axis compound parabolic concentrators. *Renewable Energy*, 1999, 16(1–4): 761–764.
- [23] Wang Y., Liu Q., Lei J., et al., A three-dimensional simulation of a parabolic trough solar collector system using molten salt as heat transfer fluid. *Applied Thermal Engineering*, 2014, 70(1): 462–476.
- [24] Hawwash A., Rahman A.K.A., Nada S., et al., Numerical investigation and experimental verification of performance enhancement of flat plate solar collector using nanofluids. *Applied Thermal Engineering*, 2018, 130: 363–374.
- [25] Li S., On the coefficient of standard deviation. *China Statistics*, 1988, (5): 32–33.
- [26] Geedipalli S.S.R., Rakesh V., Datta A.K., Modeling the heating uniformity contributed by a rotating turntable in microwave ovens. *Journal of Food Engineering*, 2007, 82(3): 359–368.
- [27] Zhang M., Ai Y., Zhang S., et al., Effect of different layout schemes on temperature uniformity of cold storage. *Jiangsu Agricultural Sciences*, 2020, 48(2): 210–221.